Desalination and Water Treatment
www.deswater.com

doi: 10.5004/dwt.2018.22020

105 (2018) 273–281
February

Biosorptive removal of uranium(VI) from aqueous solution by *Myriophyllum spicatum*

Zheng-ji Yi[a,b], Jun Yao[b,*], Mi-jia Zhu[b], Hui-lun Chen[b], Fei Wang[b], Xing Liu[a]

[a]*Key Laboratory of Functional Metal-Organic Compounds of Hunan Province and Key Laboratory of Functional Organometallic Materials of College of Hunan Province, Department of Chemistry and Material Science, Hengyang Normal University, Hengyang 421008, China, Tel. +86734-8484932, email: yizhengji2004@126.com (Z.-j. Yi), liuxing1127@sina.com (X. Liu)*
[b]*School of Civil & Environmental Engineering, and National 'International Cooperation Base on Environment and Energy', University of Science and Technology Beijing, Beijing 100083, China, Tel. +8610-82321958, email: yaojun@ustb.edu.cn (J. Yao), zhumijia128@yeah.net (M.-j. Zhu), chenhuilun@gmail.com (H.-l. Chen), wangfei6699@gmail.com (F. Wang)*

Received 8 August 2016; Accepted 10 February 2018

ABSTRACT

Batch tests were performed to study the U(VI) biosorption process by the nonliving biomass of the aquatic macrophyte *Myriophyllum spicatum*. Effects of various operational parameters, such as contact time, pH, initial U(VI) concentration, and temperature, were investigated in detail. Results suggested that the U(VI) adsorption capacity increased with increasing initial pH from 1.0 to 7.0, and the best pH was found to be 5.0. Kinetic investigations suggested that adsorption equilibrium can be reached within 80 min and pseudo-second-order kinetic model best characterizes the biosorption behavior. The adsorption thoroughly agreed with the Langmuir isotherm and the maximum adsorption capacity was calculated to be 136.61 mg/g. Changes in free energy and enthalpy derived from the adsorption data revealed that the biosorption of U(VI) onto *M. spicatum* was spontaneous ($\Delta G^0 < 0$), endothermic ($\Delta H^0 > 0$), and thermodynamically favorable. Fourier transform infrared spectroscopy and X-ray photoelectron spectroscopy analysis indicated that hydroxyl and amino groups on the algal surface could contribute to the U(VI) biosorption process, in which complexation and ion exchange mechanisms might be involved. In conclusion, *M. spicatum* biomass could be used as a promising biosorbent to remove U(VI) contamination efficiently with high adsorption capacity and fast adsorption rate.

Keywords: Uranium; Biosorption; *Myriophyllum spicatum*; Isotherm; Kinetics

1. Introduction

Uranium is a naturally occurring element and is often found at low levels in rocks, soil, water, plants, and animals. Uranium is currently the most important chemical element in nuclear industry because it has substantial commercial application as a nuclear fuel for generating electricity. However, in uranium ore mining and milling, fuel manufacturing, fuel reprocessing, and other related activities, a substantial amount of uranium-bearing wastewater is discharged into the environment, posing a serious hazard to soils, surface, and groundwater. Hexavalent uranium [U(VI)] is highly mobile and could enter the human body through ingestion as well as through inhalation. Excessive uranium intake results in serious health problems, such as liver damage, kidney damage, cancer, and even death owing to its extensive chemical toxicity and internal irradiation [1]. The World Health Organization and United States Environmental Protection Agency recommends 30 $\mu g \cdot L^{-1}$ of uranium as the maximum allowed level in drinking water [2,3]. As uranium poses a severe risk to environmental and human health, various methods for decontamination of uranium-bearing wastewater before it is released into the environment have attracted considerable attention.

Removal of uranium contamination can be achieved through conventional physical (evaporation, ultrafiltration,

*Corresponding author.

reverse osmosis) or chemical (neutralization/precipitation, ion exchange, electrodialysis) treatment methods. However, these traditional approaches not only need high investment and operating costs but also are inefficient in low-strength effluents. Therefore, environmentalists explored cost-effective, easy-handling, high-efficiency, and environment-friendly techniques for the removal of radionuclides from wastewater.

In the past decades, biosorption has emerged as a potential alternative method for the removal of radionuclides from uranium-contaminated wastewater. Various biosorbents have been chosen for uranium removal, such as bacteria [4], fungi [5], aquatic plants [6,7], and agricultural and forestry residues [8]. Among these, certain algae have proven to be inexpensive and environment-friendly biosorbents because they are not only easily available and regenerated, but have high recovery. Moreover, only a small amount of sludge required to be treated.

Myriophyllum spicatum (*Eurasian watermilfoil*) is a submerged perennial aquatic plant that grows in lakes, ponds, and slow-moving rivers. It can adapt well to a wide range of water environment, including eutrophic, brackish, and highly alkaline water. The high density of *M. spicatum* negatively affects wildlife and fish populations and makes recreational activities impossible. Therefore, *M. spicatum* can be often considered an aquatic weed or waste product. If *M. spicatum* could be harvested, sundried, and further used to clean up uranium-polluted wastewater, then we have converted waste into something valuable. Previous investigations have reported the use of *M. spicatum* to remove various heavy metals, such as Zn, Cu, Pb, and Ni [9–12].

A previous study has also reported that living *M. spicatum* could accumulate up to 1600 mg/kg uranium because its feathered leaf structures provide a considerable surface with a significant number of uranium adsorption sites [13]. Feasibility investigation for large-scale applications suggested that the biosorption processes are more appropriate than the bio-accumulation processes in that living organisms usually need the supplementation of nutrients and thereby increase chemical oxygen demand or biological oxygen demand in wastewater. Moreover, a healthy biological population keep is difficult because of metal toxicity and other inappropriate environmental factors [14]. In this study, nonliving biomass of *M. spicatum* was used as a biosorbent to remove U(VI) from aqueous solution. In the present work, *M. spicatum* was used for U(VI) removal from an aqueous solution. Several parameters that affect U(VI) adsorption, such as medium pH, adsorbent dose, shaking time, and temperature, were studied. The adsorption kinetics, isotherms, and thermodynamics were also investigated. The possible mechanism for the adsorption of U(VI) onto *M. spicatum* biomass was also examined by Fourier transform infrared spectroscopy (FTIR), scanning electron microscopy (SEM), and X-ray photoelectron spectroscopy (XPS).

2. Materials and methods

2.1. Biosorbent source and pretreatment

M. spicatum biomass used in the present study was purchased from Honghu Liangshui Aquatic Plant Co. Ltd., Jingzhou, China. The fresh biomass (without roots) was rinsed thoroughly with running water to remove silt, sand, diatoms, and other epiphytic organisms and then cut into pieces. The sliced biomass was dried under sunlight for 3 d and subsequently dewatered at 80°C for 24 h in a drying oven. The dried biomass was pulverized into fine powder and allowed to pass through an 80-mesh-opening-size sieve. The treated biomass was placed in a desiccator for subsequent use in biosorption experiments.

2.2. Preparation of uranium stock solution

To prepare a stock U(VI) solution, 1.1792 g of U_3O_8 was dissolved in 10 mL of concentrated HCl (r = 1.18 g/mL) and 2 mL of 30% H_2O_2 in a beaker. Then, the solution was heated till dry and 10 mL HCl (r = 1.18 g/mL) was introduced. The solution was further diluted up to a total volume of 1.0 L with distilled water in a volumetric flask to obtain a U(VI) stock solution (1000 mg/L) [15]. Other concentrations of U(VI) were obtained by proper dilution according to the experimental requirements.

2.3. Batch adsorption experiments

Generally, 0.12 g of adsorbents was added to a series of 250 mL stoppered conical flasks containing 100 mL of uranium solution with the desired initial U(VI) concentrations (50–300 mg/L). The pH of the solutions was adjusted when required by adding HCl (1.0 or 0.1 M) or NaOH (1.0 or 0.1 M) and by using a pH meter. Then, these flasks were shaken on a reciprocal rotary shaker at 140 r/min for specified durations at the desired temperatures (298–318 K). The supernatants were sampled at appropriate time intervals, centrifuged at 5000´*g* for 5 min, and then used to determine residual U(VI) concentrations through standard spectrophotography [16]. The uranium removal efficiency (Ad%) and uranium adsorption capacity (Q) can be determined according to the following equations:

$$Ad\% = \frac{C_0 - C_t}{C_0} \times 100 \quad (1)$$

$$Q_t = \frac{(C_0 - C_t) \times V}{W} \quad (2)$$

$$Q_e = \frac{(C_0 - C_e) \times V}{W} \quad (3)$$

where Ad% is the U(VI) removal efficiency; Q_e and Q_t are the adsorption capacity (mg/g) at equilibrium and at time t (min), respectively; C_0, C_t, and C_e are the initial U(VI) concentration, liquid-phase U(VI) concentration at time t, and equilibrium U(VI) concentration (mg/L), respectively; V is the volume of the aqueous solution (L); and W is the mass of the adsorbent (g). All the experiments were conducted in triplicate, and the arithmetic mean values of the calculations were recorded. Blank experiments were conducted to ensure that no adsorption occurred on the walls of the glassware.

2.4. Kinetic modeling

Kinetic models are employed to describe the rate-determining step of the adsorption process. Two commonly used kinetic models, namely, pseudo-first-order and pseudo-second-order models, were selected to analyze the kinetic data and to understand the rate-determining step of U(VI) adsorption onto *M. spicatum* biomass.

The pseudo-first-order equation is a simple kinetic model describing the kinetic process of liquid–solid phase sorption [17], and its linear formula can be written as follows:

$$Q_t = Q_e(1 - e^{-k_1 t}) \tag{4}$$

where k_1 is the rate constant of the pseudo-first-order sorption (min^{-1}). Evidently, k_1 can be calculated from the slope of the plot of $\ln(Q_e - Q_t)$ vs. t.

The pseudo-second-order model based on the adsorption equilibrium capacity may be expressed in the following linear form [18]:

$$\frac{t}{Q_t} = \frac{t}{Q_e} + \frac{1}{k_2 Q_e^2} \tag{5}$$

where k_2 is the rate constant of pseudo-second-order adsorption [g/(mg·min)]. Evidently, Q_e and k_2 can be determined experimentally by plotting t/Q_t vs. t and further linear regression analysis.

The Elovich model is a rate equation based on the adsorption capacity in linear form, which is generally expressed by the following equation [19]:

$$Q_t = \frac{1}{\beta_E}\ln(\alpha_E \beta_E) + \frac{1}{\beta_E}\ln(t) \tag{6}$$

where α_E is the initial adsorption rate [mg/(g·min)] and β_E is the desorption constant (g/mg). Evidently, a_E can β_E be determined experimentally by plotting Q_t vs. $\ln(t)$ and further linear regression analysis.

2.5. Equilibrium modeling

Three extensively used adsorption isotherm models, namely, Langmuir, Freundlich, and Temkin, were selected to correlate the experimental data and to accurately describe the adsorption isotherms. The deviation between experimentally observed and theoretically calculated data can be described by the square of the correlation coefficient (R^2).

The Langmuir model is based on the assumptions of adsorption homogeneity, such as uniformly energetic adsorption sites, monolayer surface coating, and no interactions among adsorbate molecules in neighboring sites [20]. The linear Langmuir equation can be written as follows:

$$Qe = \frac{bQ_{max}C_e}{1 + bC_e} \tag{7}$$

where Q_{max} is the maximum possible amount of metals adsorbed per unit of weight of adsorbent (mg/g) and b is a constant associated with the affinity of binding sites for metals (L/mg).

The Freundlich isotherm may be suitable for nonideal uptake onto heterogeneous surfaces involving multilayer adsorption [21]. The linear Freundlich equation can be expressed as follows:

$$Q_e = K_F C_e^{1/n} \tag{8}$$

where K_F is the Freundlich constant depicting the adsorption capacity of the adsorbent ((mg/g)(L/mg)$^{1/n}$) and n is the Freundlich exponent depicting adsorption intensity (dimensionless).

The Temkin model assumes a linear decrease in heat of adsorption along with surface coverage [22], and its linear form is written as follows:

$$Q_e = a\ln K_T + a\ln C_e \tag{9}$$

where K_T is an equilibrium parameter corresponding to the maximum binding energy (L/g) and a is a dimensionless constant related to the temperature and adsorption system. The Temkin isotherm considers the interaction between adsorbent and adsorbate and is based on the assumption that the free energy of adsorption is a function of the surface coverage.

2.6. Thermodynamic parameters of biosorption

The thermodynamic parameters, including change in free energy (ΔG^0), enthalpy (ΔH^0), and entropy (ΔS^0) related to the adsorption process can be calculated by using the following Gibbs–Helmholtz Eq. (10) and van't Hoff Eq. (11) [23]:

$$\Delta G^0 = \Delta H^0 - T\Delta S^0 \tag{10}$$

$$\ln K_L = \frac{\Delta S^0}{R} - \frac{\Delta H^0}{RT} \tag{11}$$

where R is the universal gas constant (8.314 J·mol^{-1}·K^{-1}) and T (K) is the absolute temperature, K_L (L/g) is an equilibrium constant obtained by multiplying the Langmuir constants Q_{max} and b. According to Eq. (11), the parameters ΔH^0 and ΔS^0 can be calculated from the slope and intercept of the plot of $\ln K_L$ against $1/T$.

2.7. Characterization of biosorbent

The sample of *M. spicatum* (0.12 g) exposed to 100 mL of 150 mg/L U(VI) solution at pH 5.0 for 1 h was centrifuged (5,000×*g*, 5 min) to remove all supernatants. Then, the precipitate was further dehydrated by vacuum drying. The samples before and after U(VI) biosorption were characterized by using the following three instrumental analyses. FTIR was conducted by using the NICOLET iS10 (Thermo Scientific) between 500 and 4,000 cm^{-1} and by using KBr pellets. The surface morphology of *M. spicatum* surface was determined by SEM (Model S-4800 Hitachi, Tokyo, Japan). The samples were gold-coated before SEM observation. XPS (Thermo ESCALAB 250, USA) with a monochromatic Al Kα X-ray beam (energy = 1,486.5 eV and power = 150 W) was adopted to determine the elementary composition and relative uranium content on the surface of *M. spicatum*. XPS spectra were recorded in the fixed analyzer transmission

mode with a pass energy of 20 eV and a step size of 0.1 eV and obtained at 8×10^9 Pa.

3. Results and discussion

3.1. Influence of contact time and biosorption kinetics

The effect of contact time on the adsorption of U(VI) onto *M. spicatum* is shown in Fig. 1. The adsorption was rapid in the first 30 min and reached up to 84.21% at 80 min. Given that the U(VI) uptake remained almost unchanged after 80 min, the optimum contact time was determined as 80 min in the following experiments.

The parameters of the pseudo-first-order, pseudo-second-order, and Elovich models are calculated and summarized in Table 1. The squared correlation coefficients (R^2) were 0.9341 for pseudo-first-order model and 0.9569 for Elovich kinetic model. As R^2 of these two models are much less than 0.99, neither of these two models are appropriate to describe the U(VI) biosorption kinetics by *M. spicatum* due to the obvious lack of linear correlation. By contrast, the R^2 value for the pseudo-second-order kinetic model was 0.9963 and close to 1.0, and the theoretical equilibrium adsorption capacity ($Q_{e,2}$ = 90.49 mg/g) derived from fitting was very close to the experimental equilibrium adsorption capacity ($Q_{e,exp}$ = 84 mg/g), implying that the U(VI) biosorption process could be perfectly described by pseudo-second-order kinetics equation.

The pseudo-second-order kinetic model has also been reported to fit uranium adsorption data better than that of the pseudo-first-order model [24]. The perfection of the pseudo-second-order model in predicting kinetic data suggested that the overall rate of the U(VI) biosorption process appeared to be controlled by chemical adsorption and that the adsorption behavior might involve valency forces through sharing or exchanging electrons between U(VI) ions and *M. spicatum*.

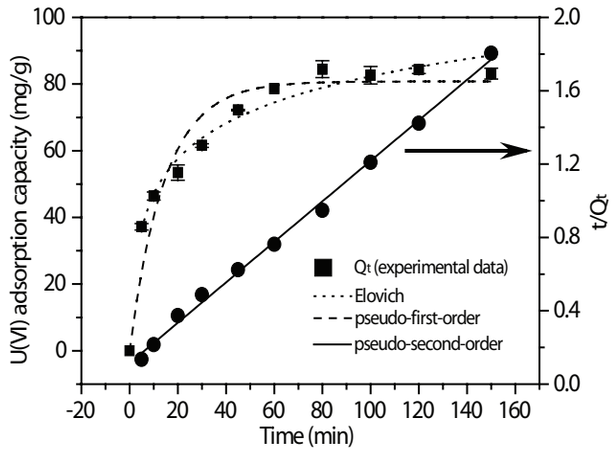

Fig. 1. Effect of time on U(VI) adsorption onto *M. spicatum* and plot of the pseudo-first-order, pseudo-second-order and Elovich kinetic equation (temperature = 298 K; pH = 5.0; U(VI) concentration = 150 mg/L; *M. spicatum* dosage = 1.2 g/L (w/v); solution volume = 100 mL).

Table 1
Kinetic parameters of U(VI) adsorption onto *M. spicatum*

Model	Parameter	Value
Pseudo-first-order	k_1 (min^{-1})	0.0691
	$Q_{e,1}$ (mg/g)	80.79
	R^2	0.9341
Pseudo-second-order	k_2 (g/(mg·min))	1.078×10^{-3}
	$Q_{e,2}$ (mg/g)	90.49
	R^2	0.9963
Elovich	α_E (mg/(g·min))	0.06491
	β_E (g/mg)	32.29
	R^2	0.9569
	$Q_{e,exp}$ (mg/g)	ca. 84

3.2. Influence of pH

The medium pH value is considered a critical parameter for biosorption system which significantly affects the protonation degree of the adsorbent as well as the existent forms of the adsorbate in the solution. The effect of pH on U(VI) adsorption was examined at different pH values ranging from 1.0 to 7.0. The uranium removal efficiency apparently increased with increasing pH from 1.0 to 5.0 and the highest U(VI) removal is achieved at pH = 5.0 (Fig. 2). Notably, at lower pH, the dominant form of uranium is uranyl (UO_2^{2+}) and the competition between H^+ and uranyl for the active functional groups (–OH, –NH_2, etc.) limits its removal. Along with the increase of pH toward neutral pH up to 5.0, these functional groups deprotonated and their chelating ability with uranyl could be enhanced, which consequently increased the U(VI) removal. On the other hand, the decrease of

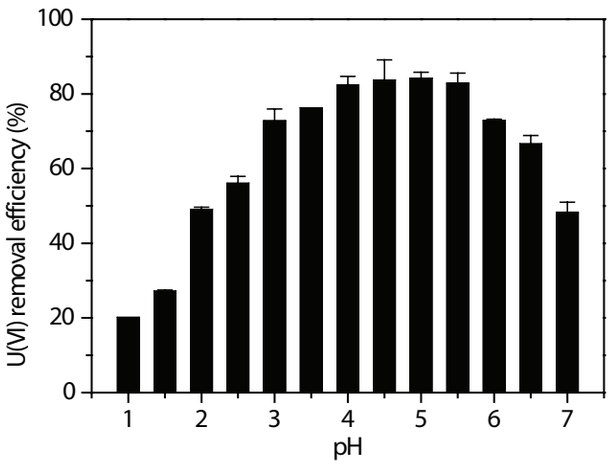

Fig. 2. Effect of pH on U(VI) adsorption onto *M. spicatum* (temperature = 298 K; contact time = 80 min; U(VI) concentration = 150 mg/L; *M. spicatum* dosage = 1.2 g/L (w/v); solution volume = 100 mL).

UO_2^{2+} and the formation of different stable monovalent uranyl species, such as $[UO_2(OH)]^+$, $[(UO_2)_2(OH)_3]^+$, and $[(UO_2)_3(OH)_5]^+$ complexes, could be responsible for the decline of the adsorption capacity [24]. The monovalent cations had greater affinity to the algal surface and they could substitute single hydrions on separate active adsorption sites. Furthermore, divalent uranyl could only replace two hydrions on the neighboring adsorption sites of the alga but could not react with those binding sites farther from one another. When the pH increased further from 5.0 to 7.0, the U(VI) removal diminished (Fig. 2). Actually, schoepite precipitation could occur at higher pH value exceeding 5.0 [26], thereby decreasing the uranium adsorption because of the decline of U(VI) concentration in solution. Therefore, the solution pH was adjusted to 5.0 in all subsequent studies to obtain the optimum adsorption efficiency.

3.3. Influence of initial U(VI) concentration and adsorption isotherm

The adsorption isotherms were employed to examine the adsorption characteristics of biosorbents via batch tests, which is useful for explaining the adsorption mechanism. To evaluate the adsorption capacity of *M. spicatum*, the initial U(VI) concentration changed from 50 mg/L to 300 mg/L. The U(VI) adsorption capacity increased with the initial concentration and reached the saturation plateau when the initial U(VI) concentration was 250 mg/L (Fig. 3).

Langmuir, Freundlich, and Temkin models were applied to correlate the adsorption data (Fig. 3). The relative adsorption parameters are shown in Table 2. The R^2 values of the plots of Langmuir, Freundlich, and Temkin isotherms showed that the Langmuir adsorption model fit best with the experimental data. Besides, the calculated value of Q_{max} (136.61 mg/g) from Langmuir equation was relatively close to the experimental value (122.24 mg/g). In consideration of the above two points, Langmuir was the best one to characterize U(VI) adsorption behavior onto *M. spicatum* among the three models. The result also revealed that the U(VI) biosorption might be considered as a monolayer adsorption on homogeneous surface, namely, having uniform adsorption energies for all the binding sites without interactions between the adsorbed metal ions.

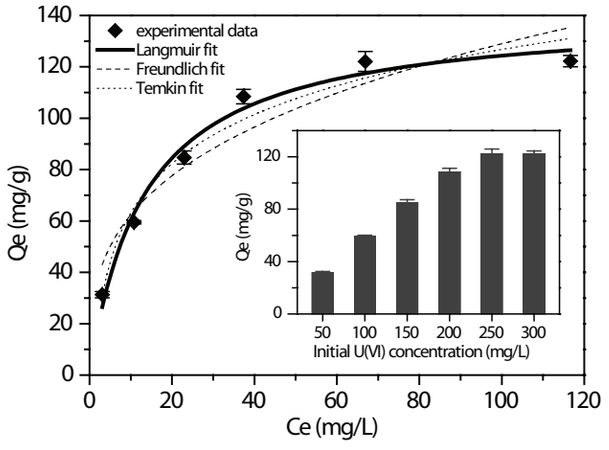

Fig. 3. Effect of initial U(VI) concentrations on its adsorption by *M. spicatum* and plot of Langmuir, Freundlich and Temkin adsorption isotherms (temperature = 298 K; contact time = 80 min; pH = 5.0; *M. spicatum* dosage = 1.2 g/L (w/v); solution volume = 100 mL).

Several other investigations have reported the Q_{max} values of some low-cost biosorbents for U(VI) adsorption (Table 3). Evidently, a comparison of these Q_{max} values showed that *M. spicatum* has greater uranium adsorption capacity than most of the other biosorbents.

A further analysis of the Langmuir equation can be conducted on the basis of a dimensionless equilibrium parameter (R_L), as given by the following equation [36]:

$$R_L = \frac{1}{1 + b \times C_0} \tag{12}$$

Table 2
Isotherm parameters for the adsorption of U(VI) onto *M. spicatum*

Model	Parameter	Value
Langmuir	Q_{max} (mg/g)	136.61
	b (L/mg)	0.0859
	R^2	0.9952
Freundlich	K_F ($mg^{(1-n)}\cdot g\cdot L^{-1}$)	30.19
	n	3.167
	R^2	0.8879
Temkin	K_T (L/g)	0.9806
	a	27.64
	R^2	0.9571

Table 3
Comparison of the U(VI) adsorption capacity with other biosorbents

Biosorbent	Q_{max} (mg/g)	Reference
Aspergillus niger	12.5	[27]
Fungus *Pleurotus ostreatus*	19.95	[28]
Biochar derived from Eucalyptus wood	27.2	[29]
Dried and pyrolyzed tea and coffee waste	59.5	[30]
Brown algae *Dictyopteris polypodioides*	62.5	[31]
Hydrilla verticillata (L.f.) Royle	78	[32]
Brown algae *Laminaria japonica*	96.4	[33]
Green algae *Cladophora hutchinsiae*	152	[34]
Trapa bispinosa	171	[35]
Myriophyllum spicatum	136.61	This research

where C_0 and b were defined previously, and R_L parameter provides information as to whether the adsorption is unfavorable ($R_L > 1$), linear ($R_L = 1$), favorable ($0 < R_L < 1$), or irreversible ($R_L = 0$). In this study, when the initial U(VI) concentration increased from 50 mg/L to 300 mg/L, the R_L value decreased from 0.189 to 0.037. Apparently, all of the R_L values are in the range of 0–1. This finding reflects that R_L values fall between 0 and 1.0 in all cases, indicative of favorable U(VI) biosorption onto the surface of *M. spicatum*.

3.4. Thermodynamic parameters

The ΔH^0 and ΔS^0 values for the adsorption process were obtained from the plot of ln K_L vs. $1/T$ and the thermodynamic parameters (ΔH^0, ΔS^0, and ΔG^0) were calculated, and the results are summarized in Table 4. The negative values of ΔG^0 demonstrated that the adsorption process was a spontaneous process over the temperature range of 288 K to 318 K. The decrease in the negative value of ΔG^0 with increasing temperature implied that the adsorption is more favorable at high temperatures. The positive ΔS^0 (30.12 J·mol^{-1}·K^{-1}) reflected the increased randomness of the adsorbed species at the solid-solution interface during the U(VI) adsorption onto *M. spicatum*. A positive ΔH^0 (4.19 kJ/mol) for this study suggested that the adsorption of U(VI) onto *M. spicatum* was an endothermic process in nature. In summary, adsorption of U(VI) on *M. spicatum* is a spontaneous, enthalpy-driven process from the thermodynamic viewpoint. These results agreed with two other studies reported on the biosorption of uranium by melanin [37] and sunflower straw [38].

3.5. Biosorbent characterization

3.5.1. FTIR spectra of M. spicatum

By comparing the FT-IR spectra of the biosorbent obtained before and after U(VI) biosorption, the functional groups on the biosorbent surface responsible for the U(VI) biosorption process were identified (Fig. 4). As for the FT-IR spectrum of raw *M. spicatum* without exposure to U(VI), the surface structure of the *M. spicatum* biosorbent was complicated and contained various functional groups. The broad absorption band near 3,271.76 cm^{-1} could be assigned to the O–H and N–H stretching vibrations, indicating that hydroxyl (–OH) and amino (–NH_2) groups were abundant on the surface of *M. spicatum*. The peaks observed at 2,924.31 and 1,417.90 might correspond to the C–H stretching vibration and scissoring vibration of methylene (–CH_2–) in the carbon chain. The peak at 1,601.59 cm^{-1} could be ascribed to the presence of C=O stretching vibrations. The intensive peak at 1,009.07 cm^{-1} could be attributed to the C–OH stretching vibration.

Table 4
Thermodynamic parameters for adsorption onto *M. spicatum*

ΔH^0 (kJ·mol^{-1})	ΔS^0 (J·mol^{-1}·K^{-1})	ΔG^0 (kJ·mol^{-1})			
		288 K	298 K	308 K	318 K
4.19	30.12	–4.48	–4.78	–5.09	–5.37

After U(VI) adsorption, the peak positions observed at 2,924.31 and 1,417.90 cm^{-1} were kept nearly constant, but their intensities weakened. This finding implied that methylene on the surface moved inside and thus it made no contribution to U(VI) adsorption. By contrast, the peaks at 3,271.76 and 1,009.07 cm^{-1} shifted to 3,292.85 and 1,011.96 cm^{-1}, respectively. This significant shifting of peak positions to higher frequency suggested that hydroxyl and amino functional groups on the biosorbent surface combined with U(VI) ions. Moreover, the characteristic peaks of hydroxyl and amino functional groups after biosorption weakened compared with those before U(VI) biosorption, which also indicated that many original free hydroxyl and amino groups might be used to adsorb U(VI) coordinatively and resulted in the decrease of their density. In general, the O atom in –OH and the N atom in –NH_2 both hybridize in the sp^3 arrangement. Two lone pairs of electrons located on the O atom and one lone pair of electrons located on the N atom can enter the empty orbital of positively charged U(VI) cations and form coordination bonds. In summary, hydroxyl and amino groups could play an important role in U(VI) biosorption.

3.5.2. SEM images of M. spicatum

Fig. 5 shows the SEM photographs of the *M. spicatum* surface before and after U(VI) biosorption. Before biosorption of U(VI), *M. spicatum* has a well-defined structure assuming rectangular texture on its surface (Fig. 5a). Although the rectangle assignment is rather regular indicative of the orderly alignment of the algal cell, the surface configuration is uneven and has concaves around all rectangles, which is favorable to the sequestration of U(VI). However, the uneven degree on the surface were reduced and somewhat disappeared after U(VI) biosorption (Fig. 5b), which implied that the concave could be filled by U(VI) due to intermolecular interaction. In other words, the *M. spicatum* surface was appropriate for the biosorption of U(VI) and a stable bond was established between the biosorbent and adsorbate.

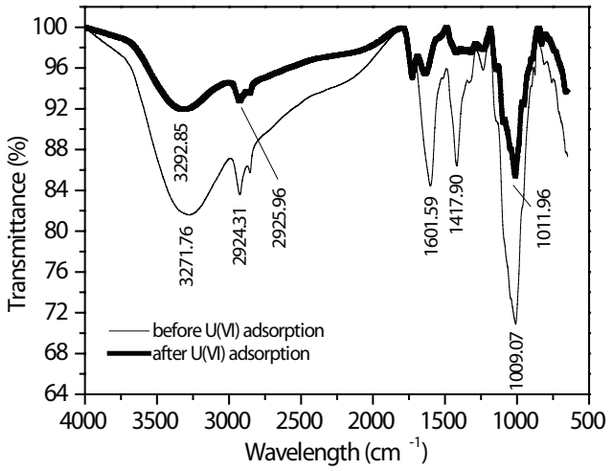

Fig. 4. FTIR spectra of *M. spicatum*: (a) before U(VI) adsorption and (b) after U(VI) adsorption.

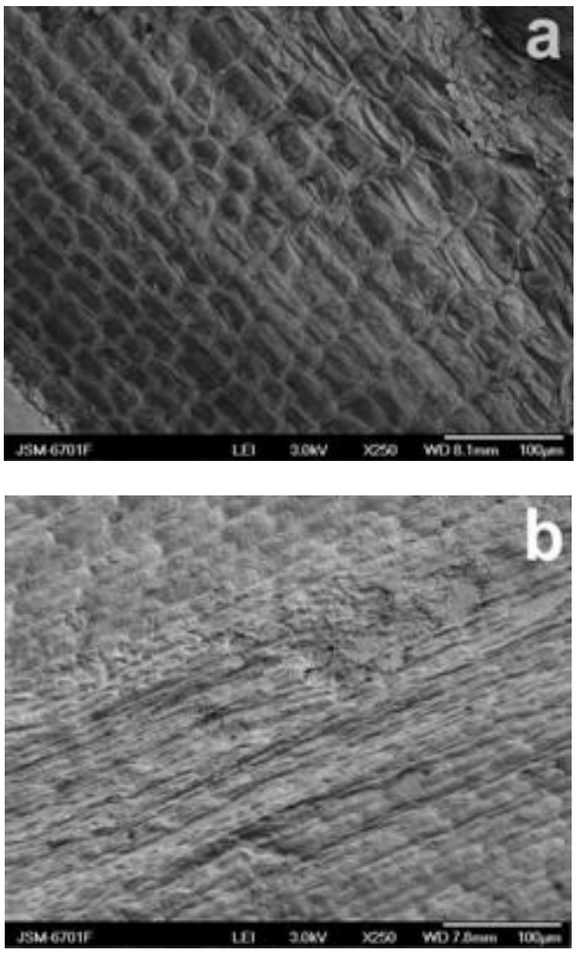

Fig. 5. SEM micrographs of *M. spicatum*: (a) before U(VI) adsorption, magnification ×250; and (b) after U(VI) adsorption, magnification ×250.

3.5.3. XPS spectra of M. spicatum

XPS is considered as a surface-sensitive quantitative tool, which can be used to determine the elemental composition and chemical state of various elements existing within a certain material. The element composition and atomic concentrations in the raw *M. spicatum* sample and after U(VI) uptake were obtained through XPS survey scan (Fig. 6 and Table 5). As for the raw *M. spicatum* sample, C, O, and N constituted three major nonmetals of *M. spicatum*; Ca, Fe, and Al are its three major metal constituents (Fig. 6a). Obviously, no U element was detected in the structural component of *M. spicatum*.

After *M. spicatum* was exposed to U(VI), the uranium signal was clearly detected (Fig. 6b). Other investigations have documented that the peaks of 4f5/2 and 4f7/2 of U(VI) were present at 392.9 ± 0.3 and 382.2 ± 0.3 eV [39, 40], respectively. In this study, the primary U4*f* peaks assigned to uranium were present at 382.18 eV for 4*f*7/2 and 392.98 eV for 4*f*5/2, both of which were in the aforementioned binding energy range. Thus, uranium remained in the unchangingly hexavalent state all through the biosorption. The two binding energy values at 382.18 and 392.98 eV reflected the bond between U(VI) ion and hydroxyl and amino groups [41,42]. The atomic concentrations of Ca, Al, and Fe were noted to drop below the detection limit after the U(VI) biosorption process. The result implied that ion exchange between U and the structural component of *M. spicatum* (Ca, Al, and Fe) could occur. According to the XPS and FTIR analyses,

Table 5
XPS atomic concentration (in percentage) of relevant chemical elements in *M. spicatum* sample before and after U(VI) uptake

Elements in the alga sample	Before U(VI) uptake	After U(VI) uptake
C	58.01	68.13
O	31.92	27.21
N	4	4.56
Si	2.86	–
Al	1.72	–
Fe	0.01	–
Ca	1.49	–
U	–	0.11

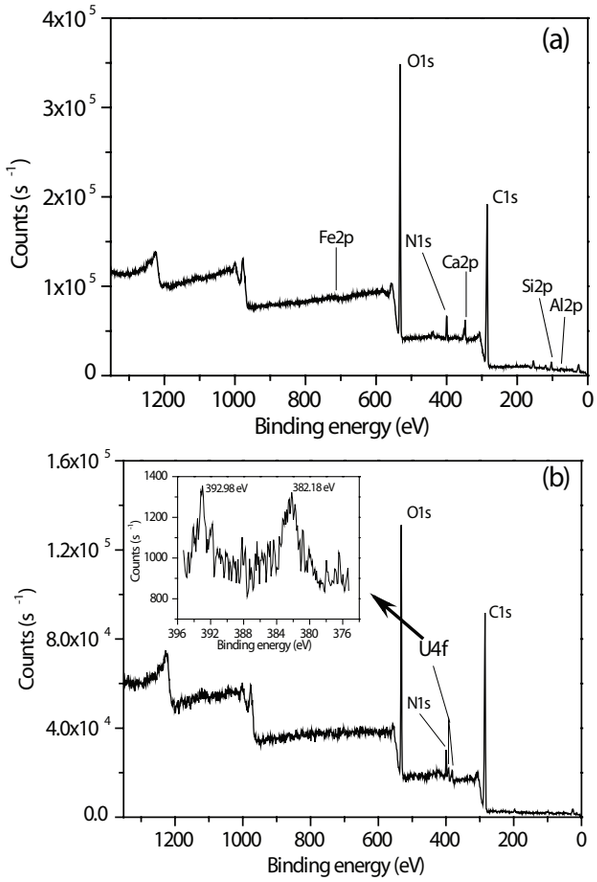

Fig. 6. XPS analysis of *M. spicatum* (a: before U(VI) adsorption; b: after U(VI) adsorption).

plus the above discussion of pH effect, we speculate that ion exchange and coordination might be two likely biosorption mechanisms responsible for U(VI) biosorption.

4. Conclusions

In this study, *M. spicatum* was found to be a promising biosorbent for the efficient removal of U(VI) from aqueous solution. The optimum pH for U(VI) removal by *M. spicatum* is 5.0. The biosorption of U(VI) onto *M. spicatum* followed Langmuir isotherm with a maximum adsorption capacity of 136.61 mg/g. The adsorption of U(VI) onto *M. spicatum* follows the pseudo-second-order model. Thermodynamic parameters, including ΔG^0, ΔH^0 and ΔS^0, indicated that the adsorption process was feasible, spontaneous and endothermic in nature. The biosorption mechanism could be explained as the dual effect of surface complexation and ion exchange. The abundant hydroxyl and amino groups on the *M. spicatum* surface may play an important role in U(VI) biosorption. On the basis of our experimental results, *M. spicatum* might also be appropriate for the removal of other metals. Therefore, more studies on the adsorption performance of *M. spicatum* towards other contaminants are ongoing in order to determine the likelihood of using it as a promising backfill material in wastewater treatment.

Acknowledgments

This work is supported in part by grants from National Natural Science Foundation of China (41773133, 21603065 and 41273131), the Key project from National Science Foundation of China (41430106), International Key Project from National Science Foundation of China (41720104007), Aid programs for Science and Technology Innovative Research Team in Higher Educational Institutions of Hunan Province and the Key Discipline of Hunan Province.

References

[1] ATSDR, Agency for Toxic Substances and Disease Registry, Toxicological profile for uranium, 2013. Available online at http://www.atsdr.cdc.gov/.
[2] WHO, World Health Organization, Uranium in drinking water, Background document for the development of WHO guidelines for drinking-water quality, WHO/SDE/WSH/03.04/118, 2011.
[3] USEPA, United States Environmental Protection Agency, Edition of the drinking water standards and health advisories, EPA 820-R-11-002, Office of Water, U.S. Environmental Protection Agency, Washington, DC, 2011.
[4] L. Sheng, J.B. Fei, Uranium adsorption by *Shewanella oneidensis* MR-1 as a function of dissolved inorganic carbon concentration, Chem. Geol., 358 (2013) 15–22.
[5] K. Akhtar, A.M. Khalid, M.W. Akhtar, M.A. Ghauri, Removal and recovery of uranium from aqueous solutions by Ca-alginate immobilized *Trichoderma harzianum*, Biores. Technol., 100 (2009) 4551–4558.
[6] A. Bampaiti, S. Yusan, S. Aytas, E. Pavlidou, F. Noli, Investigation of uranium biosorption from aqueous solutions by *Dictyopteris polypodioides* brown algae, J. Radioanal. Nucl. Chem., 307 (2016) 1335–1343.
[7] Z.J. Yi, J. Yao, H.L. Chen, F. Wang, Z.M. Yuan, X. Liu, Uranium biosorption from aqueous solution onto *Eichhornia crassipes*, J. Environ. Radioactiv., 154 (2016) 43–51.
[8] A. Lian, X.G. Luo, X.Y. Lin, S.Z. Zhang, Biosorption behaviors of uranium(VI) from aqueous solution by sunflower straw and insights of binding mechanism, J. Radioanal. Nucl. Chem., 298 (2013) 1823–1834.
[9] O. Keskinkan, M.Z.L. Goksu, A. Yuceer, M. Basibuyuk, C.F. Forster, Heavy metal adsorption characteristics of a submerged aquatic plant (*Myriophyllum spicatum*), Process Biochem., 39 (2003) 179–183.
[10] O. Keskinkan, M. Basibuyuk, Comparison of the adsorption capabilities of *Myriophyllum spicatum* and *Ceratophyllum demersum* for zinc, copper and lead, Eng. Life Sci., 7 (2007) 192–196.
[11] E. Lesage, C. Mundia, D.P.L. Rousseau, A.M.K. Van de Moortel, G. Du Laing, E. Meers, F.M.G. Tack, N. De Pauw, M.G. Verloo, Sorption of Co, Cu, Ni and Zn from industrial effluents by the submerged aquatic macrophyte *Myriophyllum spicatum L.*, Ecol. Eng., 30 (2007) 320–325.
[12] J.V. Milojkovic, M.L. Mihajlovic, M.D. Stojanovic, Z.R. Lopicic, M.S. Petrovic, T.D. Sostaric, M.D. Ristic, Pb(II) removal from aqueous solution by *Myriophyllum spicatum* and its compost: equilibrium, kinetic and thermodynamic study, J. Chem. Technol. Biotechnol., 89 (2014) 662–670.
[13] K. Aretz, E.G. Dudel, Comparison of elimination capacity of uranium from the water pathway between periphytic algae, submerse macrophytes and helophytes (emerse vascular plants), Uranium, Mining and Hydrogeology, Springer, Berlin, 2008, pp 711–712.
[14] K. Chandra Sekhar, C.T. Kamala, N.S. Chary, Y. Anjaneyulu, Removal of heavy metals using a plant biomass with reference to environmental control, Inter. J. Min. Process., 68 (2003) 37–45.
[15] Z.B. Zhang, X.F. Yu, X.H. Cao, R. Hua, M. Li, Y.H. Liu, Adsorption of U(VI) from aqueous solution by sulfonated ordered mesoporous carbon, J. Radioanal. Nucl. Chem., 301 (2014) 821–830.
[16] W.G. Chen, X.F. Zhao (Ministry of Environmental Protection of the People's Republic of China), Methods of analyzing microquantity of uranium in water, National Standard of the People's Republic of China (No. GB6768-86), (1986).
[17] S. Lagergren, About the theory of so-called adsorption of soluble substances, K. Sven. Vetenskapsakad. Handl., 24 (1898) 1–39.
[18] Y.S. Ho, G. McKay, Pseudo-second order model for sorption processes, Process Biochem., 34 (1999) 451–465.
[19] S.Y. Elovich, Mechanism of the catalytic hydrogenation of ethylene on nickel: I. Kinetics of the process, J. Phys. Chem., 13 (1939) 1761–1775.
[20] I. Langmuir, The adsorption of gases on plane surface of glass, mica and platinum, J. Am. Chem. Soc., 40 (1918) 1361–1403.
[21] H.M.F. Freundlich, Over the adsorption in solution, J. Phys. Chem., 57A (1906) 385–470.
[22] M. Temkin, V. Pyzhev, Kinetics of the synthesis of ammonia on promoted iron catalysts, J. Phy. Chem., 13 (1940) 851-867.
[23] T.S. Anirudhan, J. Nima, P.L. Divya, Adsorption and separation behavior of uranium(VI) by 4-vinylpyridine-grafted-vinyltriethoxysilane-cellulose ion imprinted polymer, J. Environ. Chem. Eng., 3 (2015) 1267–1276.
[24] S.S. Bozkurt, Z.B. Molu, L. Cavas, M. Merdivan, Biosorption of uranium(VI) and thorium(IV) onto Ulva gigantean (Kutzing) bliding: discussion of adsorption isotherms, kinetics and thermodynamic, J. Radioanal. Nucl. Chem., 288 (2011) 867–874.
[25] A.M.A. Morsy, Adsorptive removal of uranium ions from liquid waste solutions by phosphorylated chitosan, Environ. Technol. Innov., 4 (2015) 299–310.
[26] H. Zeng, A. Singh, S. Basak, K.U. Ulrich, M. Sahu, P. Biswas, J.G. Catalano, D.E. Giammar, Nanoscale size effects on uranium(VI) adsorption to hematite, Environ. Sci. Technol., 43 (2009) 1373–1378.

[27] X.Y. Wang, T.S. Wang, X.Y. Zheng, Y.H. Shen, X. Lu, Isotherms, thermodynamic and mechanism studies of removal of low concentration uranium(VI) by *Aspergillus niger*, Water Sci. Technol., 75 (2017) 2727–2736.
[28] C.S. Zhao, J. Liu, H. Tu, F.Z. Li, X.Y. Li, J.J. Yang, J.L. Liao, Y.Y. Yang, N. Liu, Q. Sun, Characteristics of uranium biosorption from aqueous solutions on fungus *Pleurotus ostreatus*, Environ. Sci. Pollut. Res., 23 (2016) 24846–24856.
[29] V. Mishra, M.K. Sureshkumar, N. Gupta, C.P. Kaushik, Study on sorption characteristics of uranium onto biochar derived from Eucalyptus wood, Water Air Soil Pollut., 228 (2017) 309.
[30] Z. Aly, V. Luca, Uranium extraction from aqueous solution using dried and pyrolyzed tea and coffee wastes, J. Radioanal. Nucl. Chem., 295 (2013) 889–900.
[31] A. Bampaiti, S. Yusan, S. Aytas, E. Pavlidou, F. Noli, Investigation of uranium biosorption from aqueous solutions by *Dictyopteris polypodioides* brown algae, J. Radioanal. Nucl. Chem. 307 (2016) 1335–1343.
[32] S. Srivastava, K.C. Bhainsa, S.F. D'Souza, Investigation of uranium accumulation potential and biochemical responses of an aquatic weed *Hydrilla verticillata* (L.f.) Royle, Biores. Technol. 101 (2010) 2573–2579.
[33] K.Y. Lee, K.W. Kim, Y.J. Baek, D.Y. Chung, E.H. Lee, S.Y. Lee, J.K. Moon, Biosorption of uranium(VI) from aqueous solution by biomass of brown algae *Laminaria japonica*, Water Sci. Technol., 70 (2014) 136–143.
[34] E. Bagda, M. Tuzen, A. Sar, Equilibrium, thermodynamic and kinetic investigations for biosorption of uranium with green algae (*Cladophora hutchinsiae*), J. Environ. Radioact. 175–176 (2017) 7–14.
[35] Z. Naseem, H.N. Bhatti, S. Sadaf, S. Noreen, S. Ilyas, Sorption of uranium(VI) by *Trapa bispinosa* from aqueous solution: effect of pretreatments and modeling studies, Desal. Water Treat., 57 (2016) 844–845.
[36] S. Tunali, T. Akar, A.S. Ozcan, I. Kiran, A. Ozcan, Equilibrium and kinetics of biosorption of lead(II) from aqueous solutions by *Cephalosporium aphidicola*, Sep. Purif. Technol., 47 (2006) 105–112.
[37] A.S. Saini, J.S. Melo, Biosorption of uranium by melanin: Kinetic, equilibrium and thermodynamic studies, Biores. Technol., 149 (2013) 155–162.
[38] M.M. Zareh, A. Aldaher, A.E.M. Hussein, M.G. Mahfouz, M. Soliman, Biosorption behaviors of uranium (VI) from aqueous solution by sunflower straw and insights of binding mechanism, J. Radioanal. Nucl. Chem., 295 (2013) 1153–1159.
[39] S. Kushwaha, B. Sreedhar, P. Padmaja, XPS, EXAFS, and FTIR as tools to probe the unexpected adsorption-coupled reduction of U(VI) to U(V) and U(IV) on Borassus flabellifer-based adsorbents, Langmuir, 28 (2012) 16038–16048.
[40] X.Q. Nie, F.Q. Dong, N. Liu, D. Zhang, M.X. Liu, J. Yang, W. Zhang, Biosorption and biomineralization of uranium(VI) from aqueous solutions by *Landoltia Punctata*, Spectr. Spectr. Anal., 35 (2015) 2613–2619.
[41] F.H. Wang, H.P. Li, Q. Liu, Z.S. Li, R.M. Li, H.S. Zhang, L.H. Liu, G.A. Emelchenko, J. Wang, A graphene oxide/amidoxime hydrogel for enhanced uranium capture, Sci. Rep., 6 (2016) 19367.
[42] Y.B. Sun, Z.Y. Wu, X.X. Wang, C.C. Ding, W.C. Cheng, S.H. Yu, X.K. Wang, Macroscopic and microscopic investigation of U(VI) and Eu(III) adsorption on carbonaceous nanofibers, Environ. Sci. Technol., 50 (2016) 4459–4467.